Flux Loss and Neutron Diffraction Measurement Ag-sheathed Bi-2223 Tapes in terms of Flux Creep

Mi-Hye Jang†

Abstract - Alternating current (AC) losses of two Bi-2223 ([Bi, Pb]: Sr: Ca: Cu: O = 2:2:2:3) tapes [(Tape I, un-twist-pitch) and the other with a twist-pitch of 10 mm (Tape II)] were measured and compared. These samples, produced by the powder-in-(Ag) tube (PIT) method, are multi-filamentary. Also, it's produced by non-twist and different twist pitch (8, 10, 13, 30, 50 and 70 mm). The critical current measurement was carried out under the environment in liquid Nitrogen and in zero-field by 4-probe method. Susceptibility measurements were conducted while cooling in a magnetic field. Flux loss measurements were conducted as a function of ramping rate, frequency and field direction. The AC flux loss increases as the twist-pitch of the tapes decreased, in agreement with the Norris Equation. Neutron-diffraction measurements have been carried out investigate the crystal structure, magnetic structures, and magnetic phase transitions in Bi-2223([Bi, Pb]:Sr:Ca:Cu:O)

Keywords: Neutron-diffraction, flux flow, flux creep, eddy current loss, AC loss, magnetization

1. Introduction

Recent achievements in the fabrication of long-length multi-filament (Bi,Pb)-Sr-Ca-Cu-O (BSCCO) high-temperature superconductor (HTS, Type II) tapes with high critical current have generated considerable interest in applications such as cables, transformers, motors and generators, and energy storage systems. Since BSCCO tapes in most large scale systems are exposed to time-varying fields (or transport alternating currents), the tapes exhibit energy dissipation mainly due to AC losses. Thus, much research has been directed toward understanding the nature and minimization of these AC losses [1-5]. In general, AC losses are dependent on the geometry of the filaments in the tapes, the magnetic and electrical properties of the superconductor, the type of matrix materials, and the amplitude and frequency of the transport current. The total losses, Q, are attributed to hysteretic loss within the filaments (Q_h), eddy current loss and coupling current loss within the matrix (Q_e), and coupling current loss across the matrix (Q_c). The Critical State model has been used extensively to describe the electrodynamics of Type II superconductors and to calculate the AC hysteresis loss [6-7]. For Bi-2223 ([Bi,Pb]:Sr:Ca:Cu:O=2:2:2:3)-based tapes consisting of multiple superconducting cores in a silver matrix, AC loss was found to be mostly frequency independent [6-8]. We have also found as other have, that the magnetic and superconducting properties are very sensitive functions of the composition. Therefore we have carried out a systematic study of the crystal structure of our samples in order to establish the systematic and identify if possible the underlying property that is controlling this very subtle dependence on composition [10].

In this paper, the AC losses of two BSCCO tapes were measured by controlling the field magnitude and the incident angles between the c-axis of the tape and the time-varying magnetic field (60 Hz). The influence of interior structure (i.e. different twist-pitch) on the transport current and AC loss was also determined. The neutron experiments were performed at the NIST Center for Neutron Research (NCNR) using the BT-7 triple axis spectrometer with a neutron wavelength of 2.47 Å provided by a pyrolytic graphite monochromator and filter.

2. Experimental Set -Up

2.1 Manufacturing of multi-filament silver sheathed Bi -2223/Ag tapes

Multi-filament silver-sheathed $Bi_{1.8}Pb_{0.4}Sr_{2.0}Ca_{2.2}Cu_{3.0}O_{10+x}$ (Bi-2223/Ag) tapes were prepared by a powder–in-tube (PIT) technique where a high c-axis grain alignment is achieved by a combination of pressing, rolling and heating [11]. To prepare Bi-2223 sample, appropriate amount of Bi_2O_3, $SrCO_3$, $CaCO_3$ and CuO were mixed and milled for 24h in methanol with ZrO_2 media. The milled slurry was dried and then calcined at 700 °C for 12 h, 800 °C for 8 h, 835 °C for 8 h, and 855 °C for 8 h. The calcinations and

† Corresponding Author: MSEL, United States Department of Commerce NIST(National Institute of Standards and Technology) 100 Bureau Drive Stop 8522 Gaithersburg, MD 20899, USA. (mhjang@nist.gov, meissner@hanmail.net)

Received 16 May, 2005 ; Accepted 21 September, 2005

grinding procedures were repeated three times. To prepare the Ag-sheathed tape, BSCCO powder was loaded into a silver tube(6.35 mm outer diameter, 4.35 mm inner diameter). The heat treatment conditions are listed in Table 1. A final additional heat treatment in the absence of oxygen was also used to ensure complete sintering and reaction of the precursor powders. Micro-structural observations were made to evaluate the uniformity of the superconductor filaments that were deformed during the twisting process.

Fig. 1 shows a schematic diagram of the apparatus used for twisting the Bi-2223/Ag multi-filament tapes. The speed of drawing (RPM) was usually between 32~2000 RPM depending on the length of the twist-pitch. During twisting, the sample was further rolled and annealed twice at 850 °C for 150h. The final multifilament Bi-2223 tapes are 51-core with Ag/Au matrix for Tape I (untwisted, density ≅ 8.05 mg/mm^3) and Ag matrix for Tape II (twist-pitch of 10 mm, density ≅ 15.91 mg/mm^3). The specifications of Tape I and Tape II are given in Table 2. The microstructure of these tapes was evaluated by optical and scanning electron microscopy (SEM) on both the polished and fractured surfaces. The degree of texturing, the twist pitch, and the presence of cracks were determined after etching the Ag sheath with a mixture of H_2O_2: NH_3 = 1:1.

Fig. 1 is schematic diagram of apparatus for twisting Bi-2223 tapes. The speed of drawing for twisting Bi-2223 multi-filament is RPM 32~2000. And samples were two times annealing when it is twisting.

Table 1 Specific characteristics of heat treatment

	Condition
Annealing rate	5 ℃/min
Annealing time	850 ℃ /150 h
Heat treatment condition	O_2 gas
Sintering rate	3.33 ℃/min

Table 2 Constant characteristics of samples

	Sample Multi-filamentary (51)	
	Tape I	Tape II
Width	4.15 mm	2.29 mm
Thickness	0.29 mm	0.15 mm
Length	7.48 mm	6.23 mm
Weight	72.49 mg	34.05 mg
Matrix	Ag-Au	Ag
Twist pitch	Non-twist	10 mm
Density	8.05200 mg/mm^3	15.91117 mg/mm^3
Filling factor	2.2	2.2

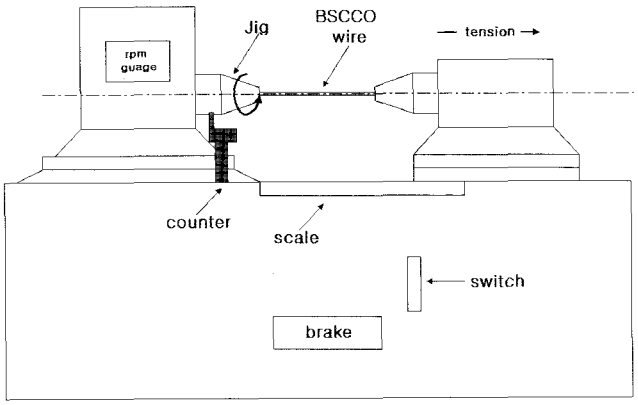

Fig. 1 Schematic diagramming of the main part of experimental apparatus used to be prepared the PIT tapes

2.2 Critical Current Measurement

Critical current (Ic) was measured by a standard four-probe technique in a zero–applied magnetic field with a 1 μ V/cm criterion. Approximately three to four specimens were tested for evaluating critical current measurement. And the critical current by applied transport current the twist pitch dependence measured at 60 Hz. The critical currents of each sample were measured at 77K under the environment with the external zero-field applied. The magnitude of external field and its incident angles to the c-axis of the sample were used as measurement variables some sample. But it was not identified, owing to its very small superconducting volume[6] of external field and its incident angles to the c-axis of the sample were used as measurement variables.

2.3 Magnetic Flux Loss Measurements

AC magnetic susceptibility was measured using a computer-controlled AC magnetometer (ACM) with AC voltage applied at a frequency of 125 Hz (harmonic 1), and external magnetic field of 10 Oe. The measurements were carried out as a function of temperature from 4.2 K to 130 K. AC losses were determined by using data measured in a superconducting quantum interference device (SQUID) magnetometer and in an AC/DC magnetometer (ACM/DCM). Fig. 2 shows the schematic drawing of the main part of the AC magnetometer. Magnetization within the sample can be determined by integrating the E.M.F. generated in the pickup coil. In these experiments, only output data from the current source of the pickup coil was used. The voltage generated by an external time-varying source was used to study the AC losses. All signals from the lock-in amplifier and data acquisition device were stored in the analog recorder. .The samples were first cooled to the lowest temperature in zero magnetic-field. The measurements were then performed in a magnetic field

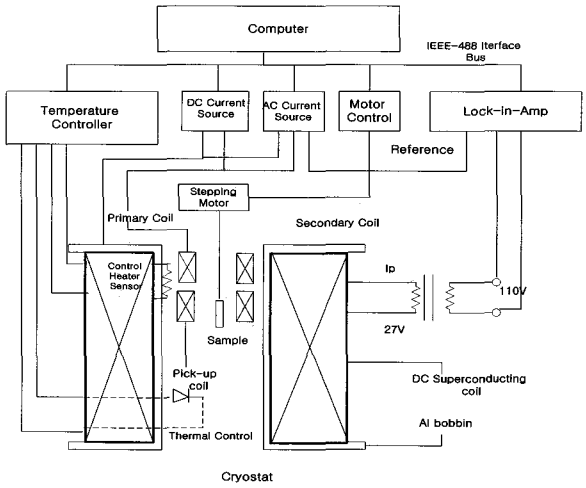

Fig. 2 Schematic drawing of experimental apparatus of main part of AC loss measurement

during warming. A change of magnetization with time while the magnetic field was applied can be explained by thermo-activated movements of vortices through the maze of pinning centers. Two types of experiments were performed to measure the flux loss. In the first type, the critical current of each sample was determined at 4.2 K, 60 K and 77 K from the peak magnetization field in the hysteresis loops. The magnitude of the external field and its incident angles to the *c*-axis of the sample were measurement variables. In the second type of experiment, AC loss measurements were carried out under constant transport current and time-varying external field of 200 Oe RMS, 1000 Hz.

2.4 The Neutron Experiment

The neutron experiments were performed at the NIST Center for Neutron Research (NCNR) using the BT-7 triple -axis spectrometer with a neutron wavelength of 2.47 Å provided by a pyrolytic graphite monochromator and filter, and the collimation before and after the sample was typically 20' full width at half maximum. The samples were held in an aluminum cylindrical holder and placed in an ILL-type top loading cryostat to cool the sample from room temperature to temperature as low as 1.6K. Lower temperatures were achieved with a cold-finger pumped [12] He cryostat (to 0.3 k). To measure the preferred crystallographic orientation of the tape we measured the (002) Bragg reflection using neutron diffraction, and since neutrons are deeply penetrating this determines the average orientation throughout the tape. To set the tape orientation, a high absorption Cd plate $5\times3\times0.2$ mm in size was mounted on one side of the tape. The detector was then moved to the straight-through position to monitor the intensity of the incident beam transmitted as the sample was rotated. The maximum in transmission should occur when the cross

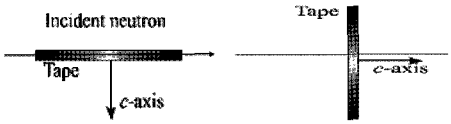

(a) Parallel setting (b) Perpendicular setting

Fig. 3 Bi2223 superconductor tape setting in the neutron diffraction experiments. (a)Tape face is parallel to the incident neutron beam; (b) tape face is perpendicular to the incident neutron beam.

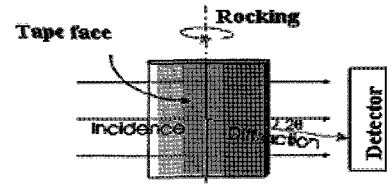

(a) Parallel setting

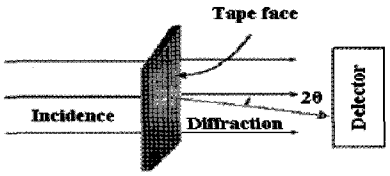

(b) Perpendicular setting

Fig. 4 Bi2223 superconductor tape setting in the neutron diffraction experiments. (a)Tape face is parallel to the incident neutron beam; (b) tape face is perpendicular to the incident neutron beam. (Diffraction)

section of the plate, and therefore the absorption, is minimized, and this maximum was chosen to define the parallel setting as shown in Fig. 3(a) and Fig. 4(a). The perpendicular setting (Fig. 3(b)) and (Fig. 4(b)) was achieved by rotating the sample table by 90 degrees. The detector was then moved to the region of 2θ=7.62°, the Bragg position for the (002) peak, and the sample angle were set to be at the nominal bisector angle for the parallel alignment. The detector was scanned through the Bragg peak, then the tape was rotated by 90° and another scanned was performed.

3. Results and Discussion

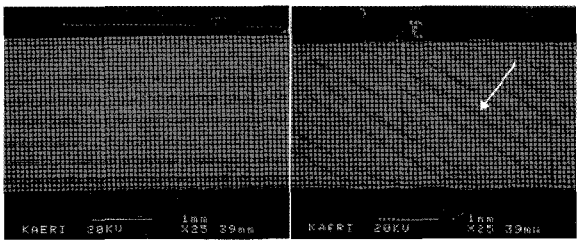

(a) Non-twisted wire (b) Twisted wire

Fig. 5 shows he microstructure of the exposed filaments for both untwisted tape (twist-pitch = ∞ mm) (Fig. 5(a)) and 10 mm (Fig. 5(b)) after etching the Ag sheath (250imes)

Micro-structural observations have been made to evaluate the uniformity of superconductor filaments deformed during the twisting process. Fig. 5 shows the SEM photo-micrographs of sheath has been completely etched away. It can be observed that exposed filaments of un-twisted wire were uniformly deformed and their interfaces were uniform and straight. Similarly, the exposed filaments of twisted wire, which were rotated 55 turns, still retained uniformity throughout the whole length of the interface was not degraded.

From the Fig. 5, it can be seen that the filaments were almost uniformly deformed for both non-twisted and twisted tapes. For twisted tapes, it is to be noted that the twist pitches were measured to be 9.7 mm, indicating that the pitches were almost the same as what we intended to obtain by calculation. In addition, the uniformity of the filaments in the twisted tapes was slightly degraded as shown in Fig.s 5(b) which can reduce the critical current mechanical strength of the tape. The mechanisms of nucleation grain growth, grain alignment, and interface chemical reaction for BSCCO superconductor phases have not clearly understood. However, several groups reported that the grain size and alignment of the BSCCO phase was larger and better near the interface between the Ag and the core than those in the center. This observation suggested that the interface plays an important role in micro-structural evolution; i.e., the interaction Ag and BSCCO [13]. It was also suggested that the interface act as a template for the grain growth and alignment are partly related to a straighter and the more uniform interface. Fig. 6 shows the critical current by applied transport current the twist pitch dependence measured at 60 Hz. From this plot it can be seen that for a given value of the low twist pitch always has the lowest critical current. For twisted tapes, it is to be noted that the critical currents were measured to be 12.34 A, 12.01 A, 11.76 A, 10.87 A, 9.60 A, 7.6 A and 6.92 A, respectively, Comparing the factors of the un-twisted, twisted 8 mm, 10 mm, 13 mm, 30 mm, 50 mm and 70 mm tapes. We find that the 10 mm twisted tapes have a greater loss factor than the un-twisted or more 13 mm twisted tapes. As a result, we can find that twisted more than 13 mm

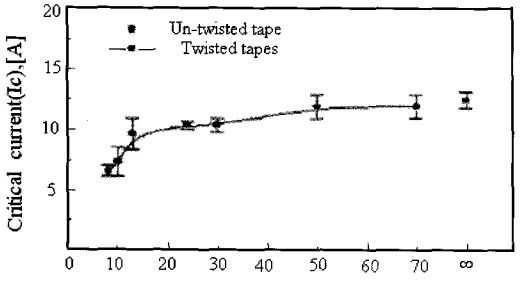

Fig. 6 Variation of critical current with various twist pitches [at 77K]

have similar to the critical current. But the critical current has drop suddenly at twisted 13 mm and less. We think the reason for this behavior does not stem from the mechanical risk and many coupling of the by electric method [at 60 Hz, 77 K].

The AC loss of each sample versus the frequency density were plotted in Fig. 7 As expected, the AC losses at an angle of 0 degree were lower than those at an angle of 90 degrees. Also, the critical current of the sample with

Ag matrix was slightly lower than that of the sample with Ag-Au matrix. The difference is too small to be on the plot scale. This is because the eddy current loss at Ag matrix is slightly larger than that at Ag-Au matrix. Fig. 7 shows the measured AC losses of each sample according to the transport current and the incident angle to the c-axis of the tape. These data include the self-hysteresis loss due to transport current. When the parallel field to the c-axis of the tape was applied, the measured loss was too larger than that due to the perpendicular field. Also, AC loss of conductor with Ag matrix and twisted was almost 2 times larger than that of conductor with Ag-Au matrix and un-twisted pitch. It is considered that this phenomenon is due to the lower critical current of the conductor with Ag matrix and twisted current of the conductor with Ag matrix and twisted included on the plot scale. This is because the eddy current loss at Ag matrix is slightly larger than that at Ag-Au matrix. It was suggested that the AC losses of filament BSCCO tape, in general, were effectively reduced when the filament size, the electrical resistivity of the matrix, and the twist pitch of the filaments were properly modified [14]. The relation between AC losses and twist pitch can be expressed by the following equations [15].

$$Qc = \frac{n\pi B^2{}_a\ \omega\tau}{\mu_o(1+\omega^2\tau^2)} \tag{1}$$

And

$$\tau = \mu_o\sigma_c L^2{}_P \frac{d^2{}_c}{16\omega^2{}_c} \tag{2}$$

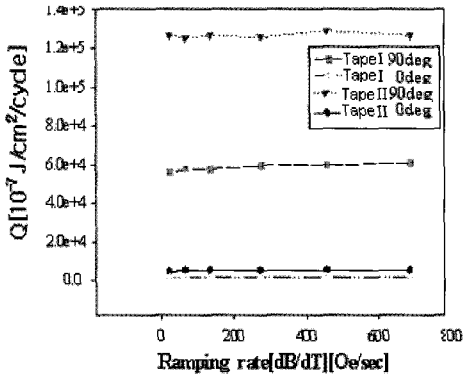

Fig. 7 Losses by magnetic field direction and ramping rate in the twisted multi-filamentary tape wire [External Magnetic Field: 1 T]

Where, Qc is the coupling current loss, n is the sharp factor, β_a is the external field amplitude, ω is the angular frequency of the field, τ is a time constant, μ is initial permeability, σ_c is the conductivity of the matrix, L_P is the twist pitch, d_c and ω_c are the thickness and width of the core, respectively. It is expected that the AC loess will decrease as the twisted pitch, according to the equation. However, the increase value in twisted pitch in the ac loss of the tape as a result of the micro-structural damages. Fig. 8 shows the measured AC losses of each sample according to the frequency and the incident angle to the c-axis of the tape. These data include the self-hysteresis loss due to transport current. When the parallel field to the c-axis of the tape was applied and at 77 K, the measured loss was too larger than that due to the perpendicular field. Also, when the parallel field to the c-axis of the tape was applied at 60 K and 4.2 K the measured loss was a few larger than that due to the perpendicular field. We didn't find out the reason why the sample have a same loss different when the parallel field and perpendicular field to the c-axis of the tape was applied and at 60 K and 4.2 K. Based on Fig. 7, and Fig. 8 equation (3), (4), (5) and (6), AC loss is magnetization due to applied field vary temperature, vary field and applied field two direction.

$$dH / dT = \frac{5 * [1.7, 0.5, 0.1,] * 10^{4}}{time\ (\min) * 60} \tag{3}$$

and

$$Qv = \frac{Q}{V} = \frac{Q}{dT * dD * dl} \tag{4}$$

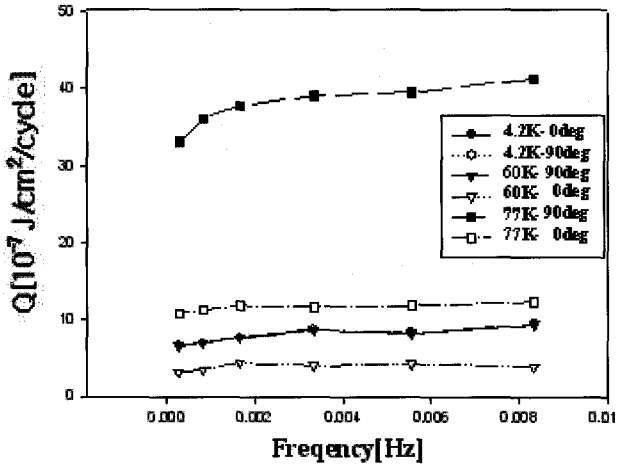

Fig. 8 AC losses according to the temperature and the incident angle to the c-axis of the tapes [non-twisted tape].

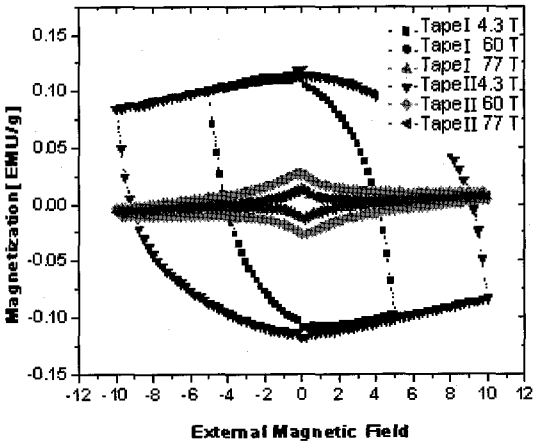

Fig. 9 Hysteresis loops depend on temperature in sheathed $Bi_{1.8}Pb_{0.4}Sr_{2.0}$ $Ca_{2.2}$ $Cu_{3.0}O_{10+}$ δ (Bi-2223/Ag);non-twisted tape, with virgin curve at 1.2 KOe

and

$$Q = \frac{1}{8} * \left(\frac{a}{b}\right)^{2} \left(\frac{L_P}{2 * 10^{9}}\right) Hm * \frac{dH}{dT} \tag{5}$$

and

$$Q = \frac{1}{8} * \left(\frac{a}{b}\right)^{2} \left(\frac{Lp^{2}}{2 * 10^{9}}\right) \frac{Hm}{\frac{\Delta Q}{\Delta \frac{dH}{dT}}} \tag{6}$$

Where, dH / dT is the magnetic field due to time varying, Q is the total loss , Qv is the loss to volume of sample, Lp is the twist pitch of core, V, a and b are the volume, width and length of the core, respectively.

Fig. 9 shows a hysteresis loop at 4.3 K, 60 K and 77 K for the two materials used for the measurements Fig. 5. For one of the materials that possessed the ability to be levitated easily by a magnet from vary temperature, sheathed $Bi_{1.8}Pb_{0.4}Sr_{2.0}Ca_{2.2}Cu_{3.0}O_{10+}$ δ (Bi-2223/Ag), the field dependence of its magnetization at 77 K, 60 K and 4.2 K after being cooled to this temperature in zero field cycles This temperature is well above the onset temperature of the superconducting 80 K phase and 15 K below the onset temperature of 110 K phase. The loop obtained would not be expected for a material simply undergoing a phase transition to a diamagnetic material but is typical for loops obtained from oxide superconductors near their onset temperatures. For this sample (density $\cong$ 8.05200 mg/mm^3, untwist) the initial small field (- 20 Oe $\leq H \leq$ + 20 Oe) loop (not show) indicated no magnetic flux penetration into the sample and had an initial sloop of – 0.078 emu/cm^3 Oe (1.3 times to the theoretical $-1/4\pi$ value for diamagnetism Flux penetration (deviation from M vs. H linearity) in

twisted 10 mm, 4.3 K, began to occur in this sample at fields near 67.6 Oe(=Hc1); from the measurable width of the (-200 Oe $\leq H \leq$ +200 Oe) loop shown in Fig. 9, flux pinning may be deduced to occur at slightly higher fields.

To measure the preferred crystallographic orientation of the tape we measured the (002) Bragg reflection using neutron diffraction, and since neutrons are deeply penetrating this determines the average orientation throughout the tape. The results of the measurements are shown in Fig. 10 and 11. This shows 2 θ scan of the (002) reflection in the parallel and perpendicular settings.

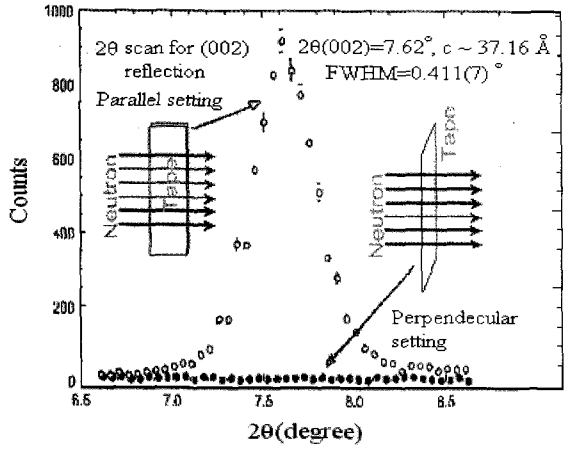

Fig. 10 2θ scan of the (002) reflection in the parallel and perpendicular settings

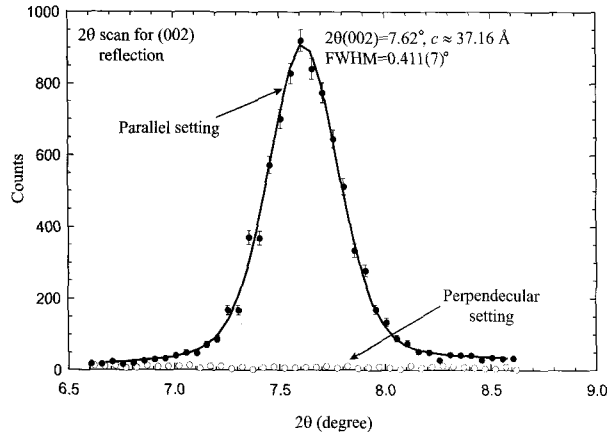

Fig. 11 The 2θ scan of the (002) reflection in the parallel and perpendicular settings. The solid curve is a fit with a Gaussian function

The detector was then moved to the region of 2θ=7.62°the Bragg position for the (002) peak, and the sample angle was set to be at the nominal bisector angle for the parallel alignment. The detector was scanned through the Bragg peak, then the tape observed. For a randomly oriented powder these two scans should have identical intensities, so these data indicate a strong preferred orientation throughout the tape.

To determine quantitatively the degree of crystallographic preferred orientation in the tape, the detector was set at the Bragg angle and the sample was rotated over a wide angular range. Fig. 12 and 13 shows this "rocking curve" for the (002) reflection. A well defined peak with the full-width-at-half-maximum of 20.7(2)° was observed at the Bragg angle of θ≈3.68°(nominally half the detector angle, as expected). A good fit to the data was achieved by using the Gaussian function. The width and distribution obtained in this measurement is a direct measurement of

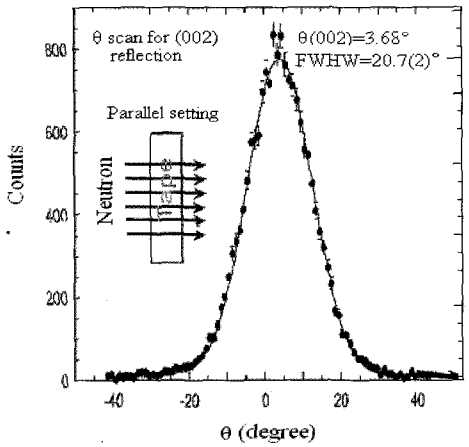

Fig. 12 Rocking curve for the (002) reflection. The solid curve is a fit with a Gaussian function

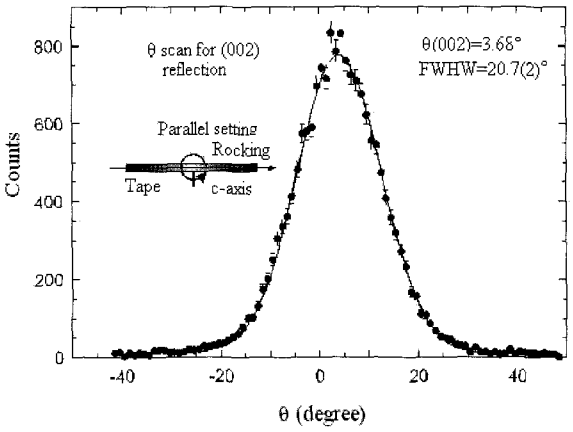

Fig. 13 Rocking curve for the (002) reflection. The solid curve is a fit with a Gaussian function.

the *c*-axis distribution of crystallites throughout the tape which is seen to provide a good representation of the data. This functional form and the observed width is a direct measurement of the *c*-axis distribution of crystallites throughout the tape. The results of the measurements are shown in Fig.10 and 11. For the 2θ-scan in the parallel setting a strong (002) peak is observed at an angle corresponding to the *c*=37.16 Å. In the perpendicular setting, on the other hand, no peak was observed. For a

randomly oriented powder these two scans should have identical intensities, so these data indicate a strong preferred orientation throughout the tape.

To determine quantitatively the degree of crystallographic preferred orientation in the tape, the detector was set at the Bragg angle and the sample was rotated over a wide angular range. Fig. 3 shows this "rocking curve" for the (002) reflection. A well defined peak with the full-width-at-half-maximum of 20.7(2)° was observed at the Bragg angle of θ≈3.68°(nominally half the detector angle, as expected). A good fit to the data was achieved by using the Gaussian function. The width and distribution obtained in this measurement is a direct measurement of the *c*-axis distribution of crystallites throughout the tape.

5. Conclusion

We have compared the loss factors of tapes with different matrix and different angles to the c-axis of the tape. From experiment, losses for fields applied parallel to the c-axis of the textured Bi-2223 grains are larger by over an order of magnitude than those applied perpendicular. For the tape, which had a twist pitch of 70 mm, approximately 64 % of the loss was maintained compared to that of the untwisted tape. The reduced may be related to interface irregularity, smaller grain size, poorer texture, and the presence of cracks caused by induced by induced strain during the twisting process. And it is confirmed that losses self-hysteresis loss due to the transport current, is currently in progress. The width and distribution obtained in this measurement is a direct measurement of the *c*-axis distribution of crystallites throughout the tape which is seen to provide a good representation of the data. This functional form and the observed width is a direct measurement of the *c*-axis distribution of crystallites throughout the tape.

Acknowledgements

This work was supported by Korea Research Grant (KRF-2004-050-D0000).Q. Huang of NIST is thanked for her assistance in the neutron experiments and Rosetta Drew of NIST is thanked for her assistance in the flux loss measurements.

References

[1] J. Yoo, J. Ko, H. Kim and H. Chung, IEEE, Trans. Appl. Supercond., 9, 2, 2163-2166,1999.

[2] Y. Yang, T. J. Hughes, and F. Duilitz, Physica C, 310, 147-153. 1998.

[3] F. Darmann, R. Zhao, G. Mcoaughey, M. Apperley, and T. P. Bealeas, C. Frieul, IEEE, Trans. Appl. Supercond., 9,[2] 89-792,1994.

[4] W. Goldaker, H. Eokkelmann, M. Quilitz, B. Ullmann, IEEE Trans. Appl. Supercond., 7.,2,1670-1673,1997.

[5] J. R. Cave, A Fe'vriev, T. Verhaege, A. Lacaze, Y. Laumond, "Reduction of AC losses in ultra-fine multi-filamentary Nb-Ti wires". IEEE Trans. Of Magnetics, Vol. 25, pp. 1945-1948, 1989

[6] M. Polak, I. Hlasnik, S. Fukui, N. Ikeda O, Tsukamoto. "Self-field effect and current-voltage characteristics of AC superconductors," Cryogenics, 34 315-324, 1994

[7] W. Swan, J. Math. Phys. 9(1968)1308

[8] W. T. Norris, "Calculation of hysteresis losses in hard superconductors carrying ac: isolated conductors and edges of thin sheets," J. Phys. D 3 489 (1970).

[9] E. H. Brandt, M. Indenbom. Phys. Rev.B48 12893-12906 (1993).

[10] H. Schmit, M. Weber, and H.F. Braun, Physica C 246,177(1995); 256,393 (1996)

[11] Jaime, M. Nunez-Regueiro, M Alario-Franco, C. Chaillout , J. J. Chenavas, B. Souletie, J. L. Tholence, S. de Brion, P. Brion, P. Bordet, M. Marezio, J. Solid State Comm., 97 131(1997)

[12] D.D. Lawrie and J. P. Frank, J. Supercond. 8, 591 (1995)

[13] J. Joo, J. P. Sighn, T.Warsyanki.Grow and R. B. Poeppel, Applied Superconductivity, 2 6 401-410 (1994)

[14] M. Jaime, M. N. Regueiro, M A.A.Franco, C. Chaillout, J.J. Capponi, A. Salpice, J. L. Tholence, S. de Brion, P. Bordet, M. Marezio, J. Chenavas, B. Souletie, Solid State Comm. 97 131(1997).9 H. Schmit, M

[15] W. J. Carr, Jr. AC loss and Macroscopic theory of superconductors 86 copyright(1983)

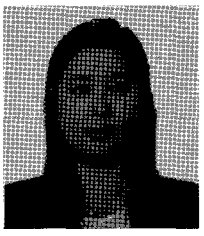

Mi-Hye Jang

She received a doctorate degree in electrical & electronic engineering from Yonsei niversity. And She has researched the Ohio State University. Also, she has been working in the United States Department of Commerce NIST National Institute of Standards and Technology since in June, 2002 Her research interests are superconducting application, diagnostic and protection system for superconducting which is also related to the AC loss and stability analysis of the superconductor. wire, Electro-magnetic properties and nano-device.
substance and nano-device.